Russian Journal of General Chemistry, Vol. 74, No. 6, 2004, pp. 908–920. Translated from Zhurnal Obshchei Khimii, Vol. 74, No. 6, 2004, pp. 983–996.

Theoretical Study of the Mechanism of the Nitro–Nitrite Rearrangement and Its Role in Gas-Phase Monomolecular Decomposition of C-Nitro Compounds

G. M. Khrapkovskii, E. V. Nikolaeva, D. V. Chachkov, and A. G. Shamov

Kazan State Technological University, Kazan, Tatarstan, Russia

Received June 13, 2002

Abstract — Semiempirical, *ab initio*, and density functional theory calculations were used to study the primary act of gas-phase monomolecular decomposition of certain C-nitro compounds and their radical cations, associated with the nitro–nitrile rearrangement. It was shown that the reaction fails to occur with all neutral molecules of aliphatic nitro compounds (except for fluoronitromethane and fluoronitroethene) and has a much lower barrier with the corresponding radical cations. An important role of the nitro–nitrile rearrangement in gas-phase decomposition of aromatic nitro compounds was demonstrated.

At present the kinetics of thermal decomposition of aliphatic and aromatic C-nitro compounds is rather well documented [1–3]. Reliable kinetic parameters are available for nearly 100 gas-phase monomolecular decomposition reactions [4, 5]. The mechanism of the primary act of gas-phase reactions is much difficult to elucidate, since here independent theoretical estimates for the energies of different alternative mechanisms are required, along with experimental data on reaction kinetics and products. Over the past years this problem has been successfully approached by *ab initio* [6, 7] and density functional theory (DFT) methods [8]. Here we present the results of a theoretical study of one of the most interesting and debated problems of thermal decomposition of nitro compounds, viz. the role of nitro–nitrite rearrangement (NNR) in gas-phase monomolecular decomposition of nitromethane, nitroethene, nitrobenzene, and their derivatives.

Initially isomerization into nitrites followed by radical or nonradical decomposition was considered as one of the possible alternative primary acts of thermal decomposition of nitro compounds, along with homolytic cleavage of the C–N bond and β-elimination of nitrous acid [1]. In succeeding years, as new data on the reaction kinetics and products became available, the results for aliphatic nitro compounds were most frequently treated in terms of the latter two mechanisms, whereas NNR attached less attention. This mechanism was also not invoked in the case of aromatic nitro compounds [3, 5].

As an alternative to the radical decomposition characteristic of nitrobenzene and most of its derivatives, processes involving isomerization of *o*-dinitrobenzene, as well as compounds with hydrogen-containing substituents (*o*-nitrotoluene, *o*-nitroaniline, *o*-nitrophenol, and their dinitro- and trinitrosubstituted analogs), followed by decomposition by different mechanisms were considered [9].

The interest in NNR was rekindled by the results of theoretical studies (primarily, for nitromethane) and mass-spectral analysis of products of high-vacuum pyrolysis of aromatic nitro compounds [10–14]. However, different quantum-chemical calculations of the rearrangement provided contradictory estimates both for the geometry of the transition state (TS) of NNR and for its energy barrier. The barrier to NNR (202 kJ mol^{-1}), calculated by the MINDO/3 method, was much lower that the C–N dissociation energy [10]. *Ab initio* (MP2, MCSCF) [11, 15] and DFT (B3LYP) [16] estimates were substantially higher (277–317 kJ mol^{-1}).

The mass spectra of products of high-vacuum pyrolysis of nitromethane contained a strong peak at *m/z* 30 (NO), that might arise from NNR [12], whereas a great body of data on the kinetics and products of initial decomposition stages provided strong evidence for a radical mechanism of the primary act [4, 5].

Similar results were obtained with aromatic nitro compounds [3, 5]. The mass spectra (electron impact

1070-3632/04/7406-0908

[14] and field ionization [6, 12, 13]) of products of high-vacuum pyrolysis of nitrobenzene and its derivatives contained strong peaks characteristic of NNR products, but the kinetic parameters of the primary act of gas-phase decomposition of aromatic nitro compounds were better consistent with a radical mechanism. Thus, for instance, high (~10^{17} s^{-1}) preexponential factors characteristic of radical decompositions were obtained for all the reactions of nitrobenzene, *m*- and *p*-dinitrobenzenes, *m*- and *p*-nitroanilines, and *m*- and *p*-nitrophenols, as well as all halonitrobenzenes studied [17, 18]. Experimental activation energies of thermal decomposition of all the above aromatic nitro compounds were almost coincident with *ab initio* estimates for the C–N dissociation energy [3, 6, 9].

Thus, the published theoretical and experimental evidence allows no unambiguous conclusions as to the possibility of NNR on gas-phase monomolecular decomposition of C-nitro compounds. First we performed *ab initio*, DFT, and semiempirical PM3 calculations (GAUSSIAN 98 [19]) for the reaction of nitromethane. The correspondence of stationary points to minima and TSs was always proved by force-constant calculations. The identification of a TS was proved by the presence of one negative value in the Gesse matrix, and its belonging to the process, by drops to reagents and products along the reaction coordinate.

The resulting TS geometries and energy barriers to NNR are presented in Tables 1 and 2, respectively. As seen, the different *ab initio* and DFT results are fairly well consistent with each other. We consider that the most reliable estimates for the energy barrier (272–275.5 kJ mol^{-1}) are provided by B3LYP/6-311++G(df,p) and B3LYP/6-31G(d) [21] calculations. As we showed previously [8], there methods give the most exact formation enthalpies and dissociation energies for nitromethane and its derivatives, as well as products of their monomolecular decomposition. As the upper limit of the energy barrier we can use the value of 284.7 kJ mol^{-1}, obtained by the QCISD/6-31G(d) method. The above values all are higher that the C–N dissociation energy in nitromethane, and, consequently, the probability of experimental observation of NNR is almost zero. In view of the fact that the TS parameters reported in [15] differ sharply from earlier reported data, as well as from our results {for example, *r*(C–N) ~362 pm [15]}, we performed a special study of NNR by the CASSCF method used in [15]. As known, CASSCF combines SCF calculations with exact account for configurational interaction (CI) for a specified orbital subset. The "active space" ($m \times n$), i.e orbitals involved in CI, was defined

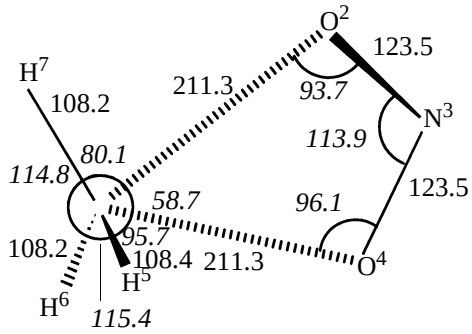

Fig. 1. Structure of the transition state of NNR as given by B3LYP/6-31G(d) calculations. Here and hereinafter, bond lengths are in pm and angles are in deg; values of angles are printed italic.

by the number of orbitals (*m*) and the quantity of electrons on them (*n*). Our calculations included (2×2), (4×4), (6×6), (8×8) active spaces. The resulting geometric parameters of the TS were qualitatively consistent with those obtained by other *ab initio* methods; as to the reaction barrier, CASSCF estimates (330–357 kJ mol^{-1}) are much higher.

It might be expected that enlarged active space in the CASSCF procedure would favor further decrease of the barrier, and in this case, provided the basis set includes all electrons, the barrier will approach other *ab initio* estimates. With increasing number of electrons and orbitals, the CASSCF procedure takes more and more time and involves oscillations, and, therefore, becomes exceedingly time- and labor-consuming.

The most important methodical conclusion from our CASSCF calculations is that the TS structure predicted by this method generally agrees with other *ab initio* results. Obviously, the TS parameters obtained in [15] by the CASSCF (2×2, 4×4)/6-31G(d) method are inconsistent with NNR. Probably, instead of NNR, a vicinity of the TS of another process was examined (as mentioned in [15], the authors failed to localize TS), since the potential surface of the isomerization and monomolecular decomposition of nitromethane is very intricate. [11]. We identified, for instance, a TS for nitromethane thermolysis with abnormally large distances between carbon and nitrogen [251.5 pm; B3LYP/6-31G(d)]. By dropping to reagents and products we found out that this TS corresponds to NNR, quite a peculiar isomerization involving oxygen exchange (Fig. 1). The structures of TSs were always tested for belonging to a specific process by drops to reagents and products along the reaction coordinate. In [15], this procedure was not performed.

Table 1. Principal geometric parameters of the transition state (*r*, pm; φ, deg) of NMR in nitromethane

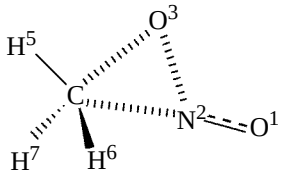

Method	Basis	C^4–N^2	N^2–O^3	N^2–O^1	O^3–C^4	$C^4N^2O^3$	$N^2O^3C^4$	$O^3C^4N^2$	$O^3N^2O^1$
PM3		183.5	128.5	118.9	188.9	72.1	67.6	40.3	120.4
HF	6-31G(d)	193.8	125.1	118.1	201.7	75.0	68.2	36.8	119.9
B3LYP	3-21G	191.1	139.0	124.8	201.8	73.4	65.2	41.3	119.6
	6-31G(d)	194.8	129.8	120.5	200.7	73.3	68.4	38.3	118.7
	6-311++G(df,p)	197.1	129.3	119.4	201.5	72.9	69.2	37.8	119.3
QCISD	6-31G(d)	193.8	130.4	120.8	208.3	75.6	69.3	37.9	115.7
CASSCF (2 × 2)	6-31G(d)	191.0	128.0	118.9	198.9	74.2	67.5	38.3	117.7
CASSCF (4 × 4)	6-31G(d)	187.3	129.5	120.0	203.7	77.7	63.9	38.4	117.0
CASSCF (6 × 6)	6-31G(d)	186.0	134.2	119.7	202.1	76.4	63.5	40.2	116.8
CASSCF (8 × 8)	6-31G(d)	189.6	129.1	121.7	204.1	77.0	64.9	38.1	117.8
MP2	6-31G(d)	181.7	135.4	122.1	190.9	72.4	65.1	42.5	118.1
	6-311++G(df,p)	180.1	132.8	120.4	187.4	71.8	65.9	42.3	119.0
MP4SQD	6-31G(d)	187.8	131.4	121.1	196.6	73.7	66.4	39.9	119.0
MINDO/3 [10]		151.6	129.9	143.8	158.4	68	–	49.5	–
MP2 [11]	6-31G(d)	192.8	125.1	118.1	203.9	–	–	–	113.0
CASSCF (4 × 4) [15]	6-31G(d)	361.7	137.1	115.5	370.0	–	–	–	–

Table 2. Activation enthalpy and heat effect of NNR in nitromethane (kJ mol^{-1})

Method	Basis	$\Delta H^{\neq}_{0\,K}$	$\Delta H^{\neq}_{298\,K}$	$\Delta H_{0\,K}$	$\Delta H_{298\,K}$
PM3		331.4	334.6	–22.6	–26.2
HF	6-31G(d)	330.9	331.3	15.6	14.6
B3LYP	3-21G	244.4	244.4	31.3	30.7
	6-31G(d)	277.5	279.1	–5.7	–6.6
	6-311++G(df,p)	272.0	272.7	–11.4	–12.5
QCISD	6-31G(d)	284.7	286.1	7.4	6.2
CASSCF (2 × 2)	6-31G(d)	332.5	332.5	22.0	21.2
CASSCF (4 × 4)	6-31G(d)	356.8	357.3	–2.5	–3.9
CASSCF (6 × 6)	6-31G(d)	321.1	321.5	–5.9	–7.2
MP2	6-31G(d)	297.3	297.1	–19.7	–20.6
	6-311++G(df,p)	297.6	297.4	–24.7	–25.9
MP4	6-31G(d)	296.8	297.1	3.3	2.2
MINDO/3 [10]		–	199.1	–	–17.2
MP2 [11]	6-31G(d)	–	307.5	–	26.8
CASSCF (4 × 4) [15]	6-31G(d)	–	287.0	–	–96.7
Experiment [20]		–	–	–	36.1

The data on substituent effects on TS geometry and reaction barrier are listed in Table 3.

For the NNR in nitroethane the calculation predicts a much lower energy barrier (by almost 17 kJ mol^{-1}). The distribution of atomic charges in the TS (Table 4) shows that methyl substitution much decreases the negative charge on the carbon atom; therewith, the charges on oxygen and nitrogen change only slightly. For this reason, attraction of the oppositely charged C and N atoms attenuates, thus attenuating repulsion of the negatively charged C and O atoms in nitroethane. Moreover, the C–O bond in the TS for nitroethane is much longer than for nitromethane (207.1 and 200.7 pm, respectively). These differences obviously explain the additional stabilization of the TS and lowering of the reaction barrier for nitroethane compared with nitromethane.

As seen from the data for dinitromethane, accumulation of nitro groups only slightly affects the energy barrier: Compared with nitromethane, the activation enthalpy decreases by ~7 kJ mol^{-1}, which is much smaller than the decrease in the C–N dissociation energy in this compound [22].

The activation enthalpies of the reactions with fluoronitromethane and chloroniteomethane are much lower than with nitromethane. Of fundamental im-

Table 3. Geometric parameters of the transition state (*r*, pm; φ, deg) and activation enthalpies of NNR in different nitroalkanes as given by B3LYP/6-31G(d) calculations (parenthesized are the geometric parameters of the initial compound)

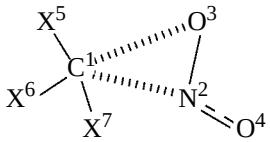

Compound	C^1–N^2	N^2–O^3	C^1–O^3	N^2–O^4	$O^3C^1N^2$	$C^1N^2O^3$	$O^3N^2O^4$	$\Delta H^{\neq}_{293\,K}$, kJ mol^{-1}
CH_3NO_2	194.8	129.8	200.7	120.5	38.3	73.3	118.7	279.1
$X^5 = X^6 = X^7 = H$	(149.9)	(122.6)	(233.7)	(122.8)	(27.7)	(117.7)	(125.9)	
CH_2FNO_2	197.8	129.6	197.9	120.4	38.2	70.9	118.8	210.9
$X^5 = X^6 = H$, $X^7 = F$	(152.1)	(121.7)	(235.7)	(122.7)	(27.0)	(118.4)	(127.7)	
CHF_2NO_2	196.7	129.2	199.4	120.3	38.1	72.1	119.4	233.9
$X^5 = H$, $X^6 = X^7 = F$	(154.0)	(121.8)	(237.0)	(122.4)	(27.0)	(118.0)	(128.2)	
CF_3NO_2	192.2	129.3	196.0	119.8	38.9	72.1	119.9	246.4
$X^5 = X^6 = X^7 = F$	(155.0)	(121.8)	(236.7)	(122.0)	(27.3)	(117.0)	(128.7)	
CH_2ClNO_2	195.2	128.3	206.3	120.4	37.1	76.1	119.5	264.9
$X^5 = Cl$, $X^6 = X^7 = H$	(152.7)	(121.6)	(238.4)	(122.7)	(26.1)	(120.3)	(127.2)	
$CHCl_2NO_2$	214.9	128.5	218.8	120.8	34.4	74.5	117.5	252.7
$X^5 = X^6 = Cl$, $X^7 = H$	(154.5)	(121.7)	(237.3)	(122.4)	(26.9)	(118.0)	(127.8)	
CCl_3NO_2	220.8	128.3	221.0	120.9	33.8	73.2	116.6	251.0
$X^5 = X^6 = X^7 = Cl$	(161.3)	(121.2)	(242.1)	(121.5)	(26.5)	(117.2)	(128.5)	
$CHFClNO_2$	203.8	128.4	210.5	120.6	36.1	74.8	119.0	248.1
$X^5 = Cl$, $X^6 = F$, $X^7 = H$	(154.1)	(122.2)	(233.3)	(121.7)	(28.4)	(114.6)	(128.3)	
CF_2ClNO_2	199.2	129.1	202.4	120.0	37.5	72.6	119.0	248.5
$X^5 = Cl$, $X^6 = X^7 = F$	(156.3)	(121.7)	(235.8)	(121.6)	(27.8)	(115.5)	(128.9)	
$CFCl_2NO_2$	208.1	128.9	209.2	120.3	36.0	72.5	117.6	250.6
$X^5 = X^6 = Cl$, $X^7 = F$	(158.3)	(121.5)	(238.0)	(121.5)	(27.3)	(115.9)	(128.9)	
CH_2BrNO_2	190.6	128.4	203.2	120.4	37.9	76.4	120.0	264.0
$X^5 = Br$, $X^6 = X^7 = H$	(152.4)	(121.7)	(238.4)	(122.7)	(26.1)	(120.4)	(127.1)	
$CH_3CH_2NO_2$	201.9	129.7	207.1	120.9	37.0	73.7	118.2	262.3
$X^5 = X^7 = H$, $X^6 = CH_3$	(151.7)	(122.6)	(236.1)	(122.7)	(27.2)	(27.2)	(125.7)	
CH_3CHFNO_2	205.1	128.2	213.1	121.2	35.6	75.6	119.0	239.7
$X^5 = F$, $X^6 = CH_3$, $X^7 = H$	(153.3)	(121.9)	(236.9)	(122.8)	(26.9)	(118.4)	(127.0)	
$CH_3CF_2NO_2$	207.9	129.2	208.7	120.8	36.1	72.3	118.1	231.4
$X^5 = X^7 = F$, $X^6 = CH_3$	(155.9)	(121.9)	(238.2)	(122.3)	(27.0)	(117.6)	(127.6)	
$CH_3CHClNO_2$	212.9	128.6	217.6	121.0	34.8	74.6	117.7	251.5
$X^5 = Cl$, $X^6 = CH_3$, $X^7 = H$	(153.1)	(122.2)	(236.0)	(122.6)	(27.3)	(117.5)	(126.6)	
$CH_3CCl_2NO_2$	222.0	128.8	221.5	121.0	33.8	72.9	116.6	246.0
$X^5 = X^7 = Cl$, $X^6 = CH_3$	(157.4)	(122.3)	(237.5)	(121.5)	(27.7)	(115.6)	(127.2)	

portance is the fact that the dissociation energy of the C–N bond in fluoronitromethane is higher than the barrier to NNR. The predicted difference between these values is small (15–17 kJ mol^{-1}), but still it implies that NNR can be observed experimentally, for which purpose the kinetics of thermal dissociation should be studied at the lowest possible temperature, since at high temperatures radical decomposition is prevailing.

From an analysis of bond lengths and bond angles in the transition and ground states for compounds whose NNR has been studied we failed to perceive why the activation energy for fluoronitromethane decreases to the greatest extent. Therefore, we focused on atomic charges in TS (Table 4).

With fluronitromethanes, the carbon and nitrogen atoms in TSs bear positive charges and the oxygen

Table 4. Atomic charges in the transition state of NNR in certain nitroalkanes as given by B3LYP/6-31G(d) calculations (in electron units)

Compound	C	N	O
CH_3NO_2	–0.293	0.300	–0.350
CH_2FNO_2	0.160	0.307	–0.368
CHF_2NO_2	0.519	0.297	–0.357
CF_3NO_2	0.897	0.318	–0.345
CH_2ClNO_2	–0.234	0.330	–0.337
$CH_3CH_2NO_2$	–0.124	0.278	–0.369
$CH_2FCH_2NO_2$	0.311	0.278	–0.369
$CHF_2CH_2NO_2$	0.685	0.279	–0.375

atom negative, whereas with nitromethane (and chloronitromethane), the nitrogen atom bears a positive charge, while carbon and oxygen are negative. Thus, the carbon and oxygen atoms in the nitromethane TS are repulsed from one another, whereas in the fluoronitromethane TSs they are attracted. As a result, the C–O bond length steadily decreases in the series nitromethane, fluoronitromethane, difluoromethane, and trifluoronitromethane. In the above series, the positive charge on the carbon atoms sharply increases, whereas on the nitrogen atom it varies only slightly. Consequently, we observe two opposite tendencies: enhancing attraction between carbon and oxygen with simultaneously enhancing repulsion between carbon and nitrogen. In the case of fluoronitromethane, attraction is prevailing, stronger stabilizing TS and much decreasing the activation enthalpy. In the case of difluoro- and trifluoronitromethanes, the positive charge on the carbon atom is very high, which enhances the role of repulsion and appreciably heighten the reaction barrier compared to fluoronitromethane.

The energy barrier for 1-fluoro-1-nitroethane is much less lowered with respect to nitroethane than for fluoronitromethane. As distinct to nitromethane derivatives, the lowest barrier is predicted for 1,1-difluoro-1-nitroethane. Analysis of changes in the geometric parameters in going from initial molecules to TSs reveals no considerable differences in the nitromethane, fluoronitromethane, difluoronitromethane and nitroethane, fluoronitroethane, difluoronitroethane series. The B3LYP/6-31G(d) charge distribution shows that the positive charge on the carbon atom of the reaction center in the TS of the reaction with fluoromethane is almost double that for the reaction with nitroethane. The additional stabilization of the TS and lowering of the reaction barrier in the case of 1,1-difluro-1-nitroethane are probably explained by interaction (attraction) between carbon and fluorine. The lowest reaction barrier to the reaction with difluronitroethane can quantitatively be explained by the fact that, unlike the reaction with difluoronitromethane, where enhanced repulsion between hydrogen and carbon takes place (according to the calculations, hydrogen bears a considerable positive charge), with difluoronitroethane this interaction is lacking, and the neighboring carbon atom (C^2) bears a negative charge in the TS, thus providing additional stabilization.

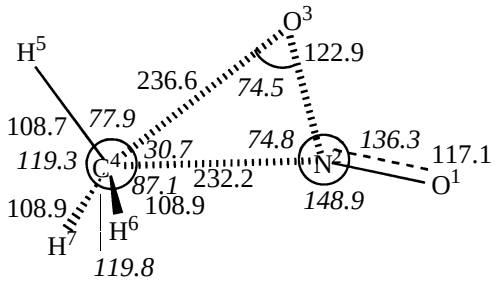

Fig. 2. Structure of the transition state of the NNR in nitromethane radical cation.

With chloronitromethanes, NNR cannot compete with radical decomposition. Firstly, accumulation of chlorine atoms sharply decreases the C–N dissociation energy (by 34 kJ mol^{-1} in chloronitromethane compared to nitromethane [23]), whereas the activation energy of NNR decreases much less (by 15 kJ mol^{-1}). Secondly, radical reactions have higher preexponential factors. As we noted above, the mass spectra at different ionization modes, as well as the mass spectra of products of gas-phase pyrolysis contain peaks assignable to NNR products: *m/z* 30 and *M* 30. Therefore, in the final part of this section we dwell on the NNR of nitromethane radical cation. The geometric parameters of the TS are shown in Fig. 2. That the TS belongs to the reagents and products was proved by the corresponding drops, and, therefore, the resulting data can be considered sufficiently reliable.

The B3LYP/6-31G(d) method used to study NNR reveals two radical cations that are close in energy but much differ in geometric parameters. The first structure (Fig. 3b) has oxygen atoms locating in the H^7CN plane and the C–N bond more than 30 pm longer and N–O bond appreciably shorter compared with the neutral molecule. This structure is obtained by dropping from the NNR transition state to the reagents and subsequent optimization. However, direct geometry optimization of nitromethane radical cation gives rise to a structure with a shortened, compared with the neutral molecule, C–N distance and oxygen atoms deviating from the H^7CN plane (Fig. 3a). This structure is more favored by energy, but the difference is as small as 21 kJ mol^{-1}. We found a TS that corresponds to interconversions of the two structures.

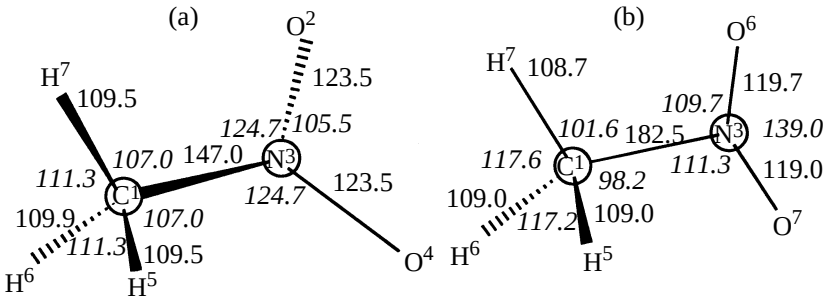

Fig. 3. Geometric structures of the (a) staggered and (b) eclipsed conformers of nitromethane radical cation as given by B3LYP/6-31G(d) calculations.

Thus, the theoretical analysis allows us to conclude that the barrier to NNR in nitromethane radical cation is much lower than in the neutral molecule (52.5 and 279.1 kJ mol^{-1} at 298.12 K). The changes in the principal geometric parameters of the reaction center in going from the initial compound to the NNR transition state for nitromethane only slightly differ from the respective values for nitromethane radical cation. For example, Δr(C–N) for nitromethane and its radical cation are 45 and 50 pm, respectively. However, the different charge distributions in nitromethane and its radical cation result in that the C–N bond in the latter gets much weaker, thus lowering the reaction barrier. In the present work we did not consider further reaction pathway and decomposition of methyl nitrite radical cation. However, the geometry and electronic structure of this species suggest that it is highly reactive and readily decomposes by different schemes.

Compared with nitroalkanes, much less attention has been paid to gas-phase reactions of nitroalkenes [4, 5]. Previously it was suggested that the primary act of monomolecular gas-phase decomposition of nitroethene and some other α-nitroolefins involves β-elimination of HNO_2 [4]. However, detailed studies of various alternative mechanisms of gas-phase decomposition of nitroethene by means of the B3LYP/6-31G(d) and B3LYP/6-311++G(df,p) methods established that the barrier to HNO_2 elimination is higher by more than 50 kJ mol^{-1} than the experimental activation energy [8]. At the same time, an alternative process was revealed, involving a cyclic intermediate (4*H*-1,2-oxazete 2-oxide), whose activation energy, with account for all possible experimental and calculation uncertainties, fairly fitted the experimental activation energy. In [24] we examined alternative further reaction pathways leading to products similar to those formed by decomposition of β-nitrostyrenes that have a structurally similar reaction center [25]; mass-spectral data for netroethenes were also invoked [26]. Table 5 lists the principal energy characteristics of the decomposition of nitroethene. As seen, the barrier to NNR in nitroethene is much lower than the C–N dissociation energy, but it is more than 42 kJ mol^{-1} higher than the activation energy of the reaction involving a cyclic intermediate.

The effect of substituents on TS geometry and reaction barrier was considered on an example of fluoronitroethenes of various structure. Certain results are presented in Table 6. Of the greatest interest is the decreased activation enthalpy for 1-fluoro-1-nitro-

Table 5. Activation parameters of initial stages of monomolecular decomposition of nitroethene as given by B3LYP calculations, kJ mol^{-1}

Process	$\Delta E^{\neq}_{0\,K}$		$\Delta H^{\neq}_{298.15\,K}$	
	6-31G(d)	6-311++G(df,p)	6-31G(d)	6-311++G(df,p)
C–N bond rupture	275.2	262.5	281.2	268.4
HNO_2 elimination	242.5	223.1	243.4	223.9
Nitro–nitrite rearrangement	241.3	237.3	241.5	237.4
1,3-H-Shift into the *aci* form	257.2	248.9	257.6	249.2
1,4-H-Shift into the *aci* form	298.8	278.8	300.3	280.2
Cyclization	202.9	205.6	201.3	203.9

Table 6. Energy barriers (kJ mol^{-1}) and transition-state structures (*r*, pm; φ, deg) for NNR in nitroolefins [B3LYP/6-31G(d)]

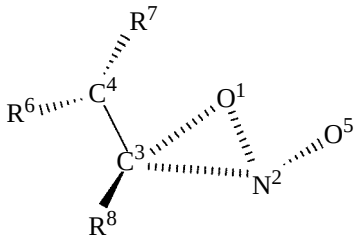

Compound	C^4–C^3	C^3–N^2	N^2–O^1	O^1–C^3	$C^4C^3N^2$	$C^3N^2O^1$	$N^2O^1C^3$	$O^1C^3N^2$	$C^4C^3N^2O^5$	$\Delta H^{\neq}_{298\,K}$, kJ mol^{-1}
$H_2C{=}CHNO_2$ $R^6 = R^7 = R^8 = H$	133.6	163.0	131.8	174.2	120.0	71.6	62.6	45.9	20.0	241.5
$H_2C{=}CClNO_2$ $R^6 = R^7 = H$, $R^8 = Cl$	133.9	162.3	132.2	174.2	119.4	71.7	62.2	46.1	23.9	236.4
$H_2C{=}CFNO_2$ $R^6 = R^7 = H$, $R^8 = F$	133.9	158.7	132.4	172.7	122.5	72.1	61.0	46.9	26.0	227.8
$HFC{=}CHNO_2$ $R^6 = F$, $R^7 = R^8 = H$	134.7	157.3	132.8	172.3	119.4	72.8	60.2	47.1	25.0	261.1
$HFC{=}CHNO_2$ $R^6 = R^8 = H$, $R^7 = F$	134.4	157.7	133.0	172.9	119.5	72.4	60.4	47.2	20.8	246.5
$HFC{=}CFNO_2$ $R^6 = R^8 = F$, $R^7 = H$	135.6	152.6	133.8	172.5	122.0	73.7	58.3	48.1	35.2	242.2
$HFC{=}CFNO_2$ $R^6 = H$, $R^7 = R^8 = F$	135.0	153.6	133.5	172.2	122.6	73.3	58.7	48.0	28.0	230.3
$F_2C{=}CHNO_2$ $R^6 = R^7 = F$, $R^8 = H$	134.8	155.7	133.5	174.1	119.7	73.6	59.1	47.3	26.0	264.9
$F_2C{=}CFNO_2$ $R^6 = R^7 = R^8 = F$	136.1	150.1	134.3	173.3	123.1	74.9	56.7	48.4	36.9	244.1

Table 7. Activation parameters of the initial stages of monomolecular decomposition of 1-fluoro-1-nitroethylene as given by B3LYP calculations, kJ mol^{-1}

Process	$\Delta E^{\neq}_{0\,K}$		$\Delta H^{\neq}_{298.15\,K}$	
	6-31G(d)	6-311++G(df,p)	6-31G(d)	6-311++G(df,p)
C–N bond rupture	262.2	246.3	267.4	251.4
HNO_2 elimination	264.1	243.9	265.2	244.8
NNR	227.5	223.6	227.8	223.7
1,4-H-shift to the *aci* form	319.3	299.1	319.4	299.2
Cyclization	222.7	223.1	221.7	221.9

ethene. With this compound we considered alternative variants of the primary act (Table 7). As seen, the barriers to NNR, predicted both by the B3LYP/6-31G(d) and B3LYP/6-311++G(df,p) methods, are close to the activation enthalpy of cyclization.

The calculated rates of these two decomposition schemes together with the activation entropies imply that in the 500–700 K range which is most convenient to study gas-phase decompositions 1-fluoro-1-nitroethene will prefer to decompose via NNR.

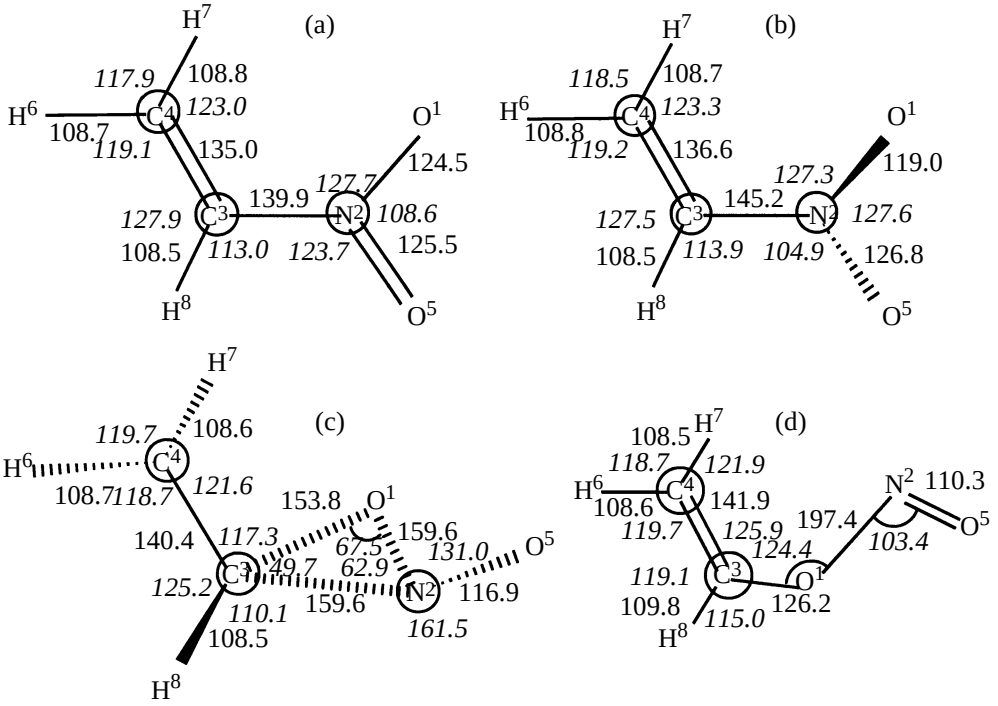

Fig. 4. Structures of (a) planar and (b) nonplanar nitroethene radical cations and transition states of the NNR in (c) nitroethene and (d) vinylnitrite radical cations.

Thus, according to the theoretical results, there are at least two alternative mechanisms of gas-phase decomposition for even the simplest nitroolefins: the process involving formation and subsequent transformation of a cyclic intermediate and NNR as the major channel of monomolecular decomposition of 1-fluro-1-nitroethene. It will also be remembered that, at temperatures of about 1000 K, radical C–N bond rupture becomes preferable because of the higher preexponential factor.

We also studied NNR in nitroethene radical cation. Like with nitromethane, the B3LYP/6-31G(d) calculation predicts two different energetically close structures (the difference in their formation enthalpies is as small as 1.6 kJ mol^{-1}): one planar and one, minimum-energy, nonplanar (the nitro group is turned with respect to the $C^4C^3N^2$ plane by about 60°). This situation is quite similar to that with nitromethane radical cation. At the same time, considerable differences are observed. First of all, as we already noted, the difference in the energies of the two structures is almost an order of magnitude smaller than with nitromethane radical cation. Moreover, it is the nonplanar structure that undergoes NNR in nitroethene radical cation. The principal geometric parameters are given in Figs. 4a and 4b.

Noteworthy is the fact the N–O bond in nitroethene radical cation is much longer than in the neutral molecule (by 4–5 and 6.5 pm in the planar and nonplanar structures, respectively). The calculation predicts a considerable asymmetry in the N–O bonds in the nonplanar radical cation. The principal TS parameters are given in Fig. 4c. Comparison of the TSs for nitroethene and nitromethane radical cations establishes that the C–N bond in the former is almost 70 pm longer than in the latter. The Δr(C–N) values (difference in C–N bond lengths in the transition and initial states) for nitromethane and nitroethene radical cations are 90 and 14.5 pm, respectively, i.e. rather strongly differ from one another.

At the same time, the barrier to NNR in nitroethene radical cation (58.4 kJ mol^{-1}) is quite close to the respective value for nitromethane radical cation (52.5 kJ mol^{-1}). These values both are five times smaller than those for the neutral molecules, implying that the radical cations will isomerize much faster and at lower temperatures.

Monomolecular gas-phase decomposition of aromatic compounds is a fairly intricate process and its kinetic parameters are very difficult to measure [2, 3, 5]. The lack of reliable theoretical estimates for the activation energies of alternative primary acts allows no firm conclusions as reaction mechanism [3, 5]. At the same time, the available kinetic evidence

Table 8. Formation enthalpies [B3LYP/6-31G(d)] and dissociation energies (D) of the C–N bond in aromatic nitro compounds (kJ mol^{-1})[a]

Compound	$\Delta H^0_{f,298\,K}$, compound	$\Delta H^0_{f,298\,K}$, radical	D(C–N)$_{298\,K}$, MP2/6-31G(d)/3-21G	D(C–N)$_{298\,K}$, B3LYP/6-31G(d)
$C_6H_5NO_2$	92.0 (68.53)	361.6 (339.8)	290.6	292.6 (285)
o-$(CH_3)C_6H_4NO_2$	76.0 (30.9)	335.0	281.7	281.9
m-$(CH_3)C_6H_4NO_2$	64.8	335.2	293.3	293.3 (278)
p-$(CH_3)C_6H_4NO_2$	63.3	337.2	293.4	296.8 (269)
o-$(NH_2)C_6H_4NO_2$	97.7	385.4	302.8	310.6
m-$(NH_2)C_6H_4NO_2$	109.9 (62.5)	381.6	298.3	294.6 (295)
p-$(NH_2)C_6H_4NO_2$	100.2 (55.2)	387.8	304.1	310.5 (302)
o-$(OH)C_6H_4NO_2$	–84.2 (–28.8)	219.0	301.3	326.1
m-$(OH)C_6H_4NO_2$	–58.2 (–105.5)	209.0	290.4	290.2 (292)
p-$(OH)C_6H_4NO_2$	–66.0 (–114.7)	214.1	294.6	303.1
o-$FC_6H_4NO_2$	–85.8	166.2	–	275.0
m-$FC_6H_4NO_2$	–108.4	155.9	–	287.3
p-$FC_6H_4NO_2$	–112.6	159.5	–	295.0
o-$ClC_6H_4NO_2$	115.1	353.4	–	261.3 (275)
m-$ClC_6H_4NO_2$	85.2	347.5	–	285.2 (287)
p-$ClC_6H_4NO_2$	82.2	350.4	–	291.2 (294)
o-$BrC_6H_4NO_2$	133.2	373.6	–	263.4
m-$BrC_6H_4NO_2$	106.6	368.7	–	285.1 (291)
p-$BrC_6H_4NO_2$	104.0	371.8	–	290.8(297)
o-$(NO_2)C_6H_4NO_2$	126.5	348.3	–	244.8
m-$(NO_2)C_6H_4NO_2$	83.0	340.8	–	280.8 (278)
p-$(NO_2)C_6H_4NO_2$	83.6	340.3	–	279.7(280)
symm-$C_6H_3(NO_2)_3$	87.0	335.0 NO_2: 23.0 (33.1)	–	271.0 (275)

[a] Parenthesized are experimental activation energies of gas-phase decomposition [5].

allows the gas-phase decomposition to be reliably treated in terms of two principal mechanisms. The activation energies for nitrobenzene, its halo derivatives, as well as *meta*- and *para*-substituted nitrotoluenes, nitroanilines, and nitrophenols are fairly close to each other and vary in parallel with C–N bond strength (Table 8). This fact leads us to expect that the primary act of the decomposition of these two compounds is associated with NO_2 elimination.

The activation energies and preexponential factors for gas-phase decompositions of onitrotoluene, *o*-nitroaniline, *o*-nitrophenol, and their nitro derivatives are much lower and uncharacteristic of radical reactions.

Our MP2/6-31G//3-21G *ab initio* study of the mechanisms of thermal decomposition of aromatic nitro compounds [6, 9] showed that the experimental activation energies are close to the energy barrier to hydrogen transfer from a hydrogen-containing substituent to an oxygen atom of the NO_2 group. Secondary thermolysis reactions of aromatic nitro compounds were found to involve an energetically favorable $^{\cdot}OH$ elimination process in the rearrangement products, which may explain the further reaction pathway. The $^{\cdot}OH$ formation was detected in the mass spectra of high-vacuum pyrolysis products of *o*-nitrotoluene, *o*-nitroaniline, *o*-nitrobenzene, and their dinitro derivatives [6, 12, 13]. Thus, the kinetic results are fairly consistent with the mass-spectral and theoretical data and point to a molecular mechanism of the primary act of the decomposition of the corresponding compounds.

Therewith, the role of NNR has so far been unclear. As noted above, the mass spectra of nitrobenzene, halonitrobenzenes, and some other aromatic nitro compounds contained fairly abundant NO ion peaks (*m/z* 30) assignable to NNR. We performed a theoretical study of the TS structure and the energy barrier to this reaction for a broad range of aromatic nitro compounds.

The principal geometric parameters of the TS and the energy barriers to NNR of nitrobenzene, its

Table 9. Geometric parameters of the transition state (*r*, pm; φ, deg) and activation enthalpies of the NNR in aromatic nitro compounds[a]

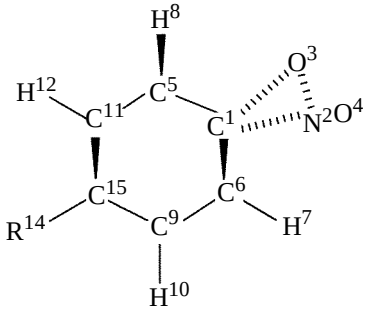

Compound	C^1–N^2	N^2–O^3	C^1–O^3	N^2–O^4	$O^3C^1N^2$	$C^1N^2O^3$	$O^3N^2O^4$	$\Delta H^{\neq}_{293\,K}$, kJ mol^{-1}
Nitrobenzene	169.2	131.7	178.2	120.7	44.5	71.4	120.9	263.6
o-Nitrotoluene	168.0	131.9	178.8	120.8	44.6	72.1	120.8	243.5
m-Nitrotoluene	169.4	131.7	178.4	120.8	44.4	71.5	120.8	263.2
p-Nitrotoluene	167.8	132.0	177.9	120.9	44.8	71.6	120.7	266.5
o-Nitroaniline	159.0	132.9	180.4	123.5	45.6	75.7	119.3	264.9
m-Nitroaniline	169.4	131.7	178.0	120.7	44.5	71.2	120.9	263.2
p-Nitroaniline	163.6	132.9	177.5	121.6	45.6	72.7	120.3	276.1
o-Nitrophenol	166.3	133.3	181.5	121.0	44.8	73.7	120.1	282.9
m-Nitrophenol	169.4	131.6	177.6	120.6	44.5	71.1	121.0	261.9
p-Nitrophenol	165.2	132.6	177.5	121.2	45.3	72.2	120.6	273.2
o-Dinitrobenzene	164.8	131.9	169.5	119.4	46.4	68.7	122.9	223.0
m-Dinitrobenzene	168.8	131.6	176.5	120.1	44.8	70.7	121.5	261.1
p-Dinitrobenzene	168.2	131.3	174.9	120.0	44.9	70.2	122.2	251.5
1,3,5-Trinitrobenzene	168.7	131.5	175.1	119.7	44.9	70.1	122.3	256.9
o-Fluoronitrobenzene	165.2	132.6	175.7	120.5	45.7	71.3	121.2	283.3
m-Fluoronitrobenzene	169.0	131.6	177.2	120.4	44.6	71.0	121.2	262.3
p-Fluoronitrobenzene	167.1	132.1	177.4	120.8	45.0	71.7	120.8	269.5

[a] R^{14} = H for nitrobenzene, R^{14} = CH_3 for *p*-nitrotoluene, and R^{14} = NH_2 for *p*-nitroaniline.

monofunctional derivatives, and 1,3,5-trinitrobenzene are given in Table 9. With all the compounds studied, the activation energy of NNR proved to be lower than the C–N dissociation energy, implying that NNR can contribute into the total gas-phase decomposition rate constant. The energy barrier to NNR varies in parallel with C–N dissociation energy in all the compounds studied. The lowest energy barriers are characteristic of *o*-dinitrobenzene and *o*-nitrotoluene.

Comparison of the geometric parameters of the TS and the initial molecules shows that *o*-dinitrobenzene and *o*-nitrotoluene exhibit the smallest changes in bond lengths in going from the initial molecule to TS. Thus the Δr(C–N) values for *o*-dinitrobenzene and *o*-nitrotoluene are 17.3 and 20.5 pm, whereas the respective value for nitrobenzene is 30 pm. With accumulation of nitro groups, as seen from a comparison of nitrobenzene, *m*-dinitrobenzene, and 1,3,5-trinitrobenzene, the reaction barrier slightly lowers (by 6.7 kJ mol^{-1}). The Δr(C–N) values for these compounds are 21.9, 21.1, and 20.8 pm, respectively. The tendency of the barrier to NNR to decrease with accumulation of nitro groups is even less pronounced than the tendency of the C–N bond to weaken: by 21.7 kJ mol^{-1} along the nitrobenzene, *m*-dinitrobenzene, and 1,3,5-trinitrobenzene series [B3LYP/6-31G(d) data]. Therefore, the contribution of NNR into the total gas-phase decomposition rate constant for mononitrobenzenes should be larger than for polynitrobenzenes.

With the resulting calculated activation entropies, energy barriers to NNR, and C–N dissociation energies, as well as experimental preexponential factors, one can estimate the relative rates of radical

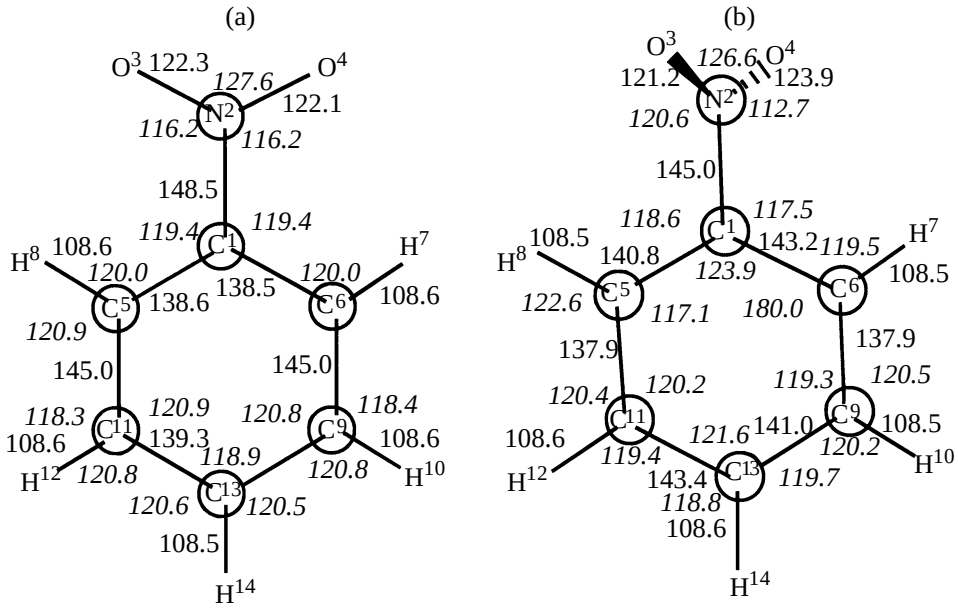

Fig. 5. Structures of nitrobenzene radical cation as given by B3LYP/6-31G(d) calculations: (a) planar and (b) nonplanar (the NO_2 group is turned with respect to the ring plane by about 50°).

and molecular decompositions. We performed such calculations for nitrobenzene at different temperatures. At 298.15 K, the contribution of NNR into the total decomposition rate constant will prevail. With increasing temperature, this ratio will change in favor of the radical mechanism. At 600 K, the rate ratio of the radical decomposition and NNR is 4.95. But here, too, the contribution of NNR into the total rate constant is not negligible. The resulting data give us grounds to state that kinetic parameters corresponding to the primary act should be measured at ashigh-as-possible temperatures (above 750–800 K), when the contribution of NNR into the total rate constant can be neglected.

Analysis of available data on the kinetics of gas-phase decomposition of nitrobenzene and its simplest derivatives shows that NNR contributes much in the case of *p*- and *m*-nitrotoluenes that were studied at 653–723 and 673–743 K [5], i.e. at lower temperatures than other nitrobenzene derivatives. As we mentioned in [6, 27], the published activation energies of gas-phase decomposition of *p*- and *m*-nitrotoluenes seem inconsistent with a radical primary act. In [27], in particular, we found correlations between the changes in the length of the ruptured C–N bond and the activation energy of gas-phase decomposition of these compounds that presumably decomposed by a radical mechanism; therewith, points for nitrotoluenes deviated strongly from this correlation dependence. The same conclusions follow from the C–N dissociation energies estimated by the MP2/6-31G//3-21G and B3LYP/6-31G(d) methods (Table 8). As seen, the *D*(C–N) values for nitrotoluenes are slightly higher than for nitrobenzene.

One of the possible explanations for the deviation of the kinetic parameters of gas-phase decomposition of *m*- and *p*-nitrotoluenes from values expected for a radical primary act is that the total reaction rate constant for nitrotoluenes (first of all, *p*-nitrotoluenes) is contributed, along with the radical mechanism of the primary act, by the concurrent NNR.

Taking into account that over the past few years much emphasis has been paid to mass-spectral studies of thermolysis of aromatic nitro compounds, as well as to decomposition of nitrobenzene and its derivatives under electron impact and other ionizations, we also considered the NNR of nitrobenzene radical cation.

Figures 5a and 5b show the structures of nitrobenzene radical cations. In the minimum-energy structure, the NO_2 group is turned by 55.5° with respect to the ring plane. The planar radical cation is 7 kJ mol^{-1} higher in energy, and its geometric parameters are close to those of the neutral molecule. It was established that isomerization associated with NNR can only occur in the nonlanar radical cation. The structure of the TS of the corresponding process is shown in Fig. 6. The activation energy is 114.2 kJ mol^{-1}.

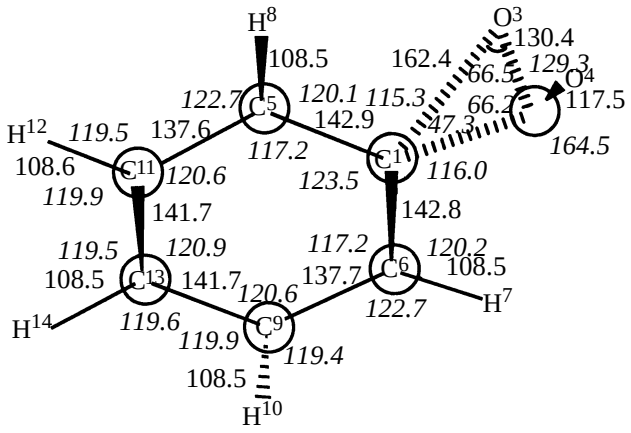

Fig. 6. Structure of the transition state of the NNR in nitrobenzene radical cation as given by B3LYP/6-31G(d) calculations.

The C–N and N–O bond lengths in the TS only slightly differ from those in the initial state. Therefore, the reaction has a much lower activation energy. Thus, according to the calculation, nitrobenzene radical cation fairly readily isomerizes into nitrites. This is a possible reason for the observation of abundant peaks of NO (*m/z* 30) in the electron impact and field ionization mass spectra of products of gas-phase pyrolysis of nitrobenzene.

In the present work we do not discuss such a fairly complicated problem as interpretation of the mass spectra of products of high-temperature pyrolysis of nitrobenzene and some other aromatic nitro compounds. At the same time, it is quite obvious that in interpreting the corresponding data one should account for NNR involving radical cations.

Our advanced nonempirical and DFT study established that NNR can compete with other mechanisms of gas-phase monomolecular decomposition of certain nitroalkanes (such as fluoronitromethane), nitroalkenes (such as 1-fluoro-1-nitroethene), and aromatic nitro compounds. This finding opens the way to experimental determination of the reaction barrier. Moreover, the competition of different mechanisms of the monomolecular decomposition should be taken into account in experimental determination of the activation energies of the primary act of radical gas-phase decomposition of nitro compounds and estimation from these data of C–N dissociation energies, primarily for aromatic nitro compounds.

ACKNOWLEDGMENTS

The work was financially supported by the Competitive Center for Basic Natural Science at the Ministry of Education of the Russian Federation (project no. E00-5.0-311) and Russian Foundation for Basic Research (project no. 3-07-90 092).

REFERENCES

1. Nazin, G.M., Manelis, G.B., and Dubovitskii, F.I., *Usp. Khim.*, 1968, vol. 37, no. 8, p. 1443.
2. Andreev, K.K., *Termicheskoe razlozhenie i gorenie vzryvchatyh veschestv* (Thermal Decomposition and Combustion of Explosives), Novosibirsk: Nauka, 1966.
3. Brill, T.B. and James, F.J., *Chem. Rev.*, 1993, vol. 93, p. 2667.
4. Nazin, G.M. and Manelis, G.B., *Usp. Khim.*, 1994, vol. 63, no. 4, p. 327.
5. Manelis, G.B., Nazin, G.M., Rubtsov, Yu.I., and Strunin, V.A., *Termicheskoe razlozhenie i gorenie vzryvchatyh veschestv* (Thermal Decomposition and Combustion of Explosives), Moscow: Nauka, 1996.
6. Khrapkovskii, G.M., Marchenko, G.N., and Shamov, A.G., *Vliyanie molekulyarnoi struktury na kineticheskie parametry monomolekulyarnogo raspada S- i O-nitrosoedinenii* (Effect of Molecular Structure on the Kinetic Parameters of Monomolecular Decomposition of C- and O-Nitro Compounds), Kazan: FEN, 1997.
7. Khrapkovskii, G.M., Shamov, A.G., Shamov, G.A., and Shlyapochnikov, V.A., *Mendeleev. Commun.*, 1997, no. 5, p. 169.
8. Shamov, A.G. and Khrapkovskii, G.M., *30th Int. Annual Conf. of ICT*, Karlsruhe, 1999, p. 60, pp. 1–14.
9. Khrapkovskii, G.M., Shamov, A.G., Shamov, G.A., and Shlyapochnikov, V.A., *Zh. Org. Khim.*, 1999, vol. 35, no. 6, p. 891.
10. Dewar, M.J.S., Ritchie, P., and Alster, J., *J. Org. Chem.*, 1985, vol. 50, p. 1031.
11. McKee, M.L., *J. Am. Chem. Soc.*, 1986, vol. 108, p. 5784.
12. Kolosov, V.D., Klimenko, G.K., Pankrushev, Yu.A., and Osipov, G.A., Abstracts of Papers, *IV Vsesoyuznoe simpozium po goreniyu i vzryvu* (IV Russian Conf. on Combustion and Explosion), Moscow: Nauka, 1977, p. 549.
13. Kolosov, V.D., Klimenko, G.K., Pankrushev, Yu.A., Osipov, G.A., Khrapkovskii, G.M., and Stolyarov, P.N., *Khimicheskaya fizika goreniya i vzryva. Kinetika khimicheskih reaktsii* (Chemical Physics of Combustion and Explosion. Kinetics of Chemical Reactions), Proc. V Russian Symp. on Combustion and Explosion, Moscow: Chernogolovka, 1977, p. 54.
14. Korsunskii, B.L., Nazin, G.M., Stepanov, V.R., and Fedotov, A.A., *Kinet. Katal.*, 1993, vol. 34, no. 8, p. 775.

15. McKee, M.L., *J. Phys. Chem.*, 1989, vol. 93, p. 7365.
16. Shamov, A.G., Shamov, G.A., and Khrapkovskii, G.M., in *Struktura i dinamika molekulyarnyh system* (Structure and Dynamics of Molecular Systems), Ioshkar-Ola, 1998, issue IV, vol. 3, pp. 183–187.
17. Matveev, V.G., Dubikhin, V.V., and Nazin, G.B., *Izv. Akad. Nauk SSSR, Ser. Khim.*, 1978, p. 783.
18. Gonzalez, A.C., Larson, C.W., McMillan, D.E., and Golden, D.B., *J. Phys. Chem.*, 1985, vol. 89, p. 4809.
19. Frisch, M.J., Trucks, G.W., Schlegel, H.B., Scuseria, G.E., Robb, M.A., Cheeseman, J.R., Zakrzewski, V.G., Montgomery, J.A., Stratmann, R.E., Jr., Burant, J.C., Dapprich, S., Millam, J.M., Daniels, A.D., Kudin, K.N., Strain, M.C., Farkas, O., Tomasi, J., Barone, V., Cossi, M., Cammi, R., Mennucci, B., Pomelli, C., Adamo, C., Clifford, S., Ochterski, J., Petersson, G.A., Ayala, P.Y., Cui, Q., Morokuma, K., Malick, D.K., Rabuck, A.D., Raghavachari, K., Foresman, J.B., Cioslowski, J., Ortiz, J.V., Baboul, A.G., Stefanov, B.B., Liu, G., Liashenko, A., Piskorz, P., Komaromi, I., Gomperts, R., Martin, R.L., Fox, D.J., Keith, T., Al-Laham, M. A., Peng, M.A., Nanayakkara, A., Gonzalez, C., Challacombe, C., Gill, P.M.W., Johnson, B., Chen, W., Wong, M.W., Andres, J.L., Gonzalez, C., Head-Gordon, M., Replogle, E.S., and Pople, J.A., *GAUSSIAN 98*, Pittsburgh: Gaussian, 1998.
20. *Molekulyarnie postoyannie neorganicheskih soedinenii: Spravochnik* (Molecular Constants of Inorganic Compounds: Handbook), Krasnov, K.S., Ed., Leningrad: Khimiya, 1979.
21. Nikolaeva, E.V., Shamov, A.G., and Khrapkovskii, G.M., *Struktura i dinamika molekulyarnyh system* (Structure and Dynamics of Molecular Systems), Moscow, 2000, pp. 447–450.
22. Karapet'yants, M.Kh. and Karapet'yants, M.L., *Osnovnye termodinamicheskie konstanty neorganicheskih i organicheskih veschestv* (Principal Thermodynamic Constants of Inorganic and Organic Substances), Moscow: Khimiya, 1969.
23. Khrapkovskii, G.M., Chachkov, D.V., and Shamov, A.G., *Zh. Obshch. Khim.*, 2001, vol. 71, no. 9, p. 1530.
24. Shamov, A.G. and Khrapkovskii, G.M., *Mendeleev. Commun.*, 2001, no. 4, p. 163.
25. Kinstle, T.H. and Stam, J.G., *J. Org. Chem.*, 1970, vol. 35, p. 1771.
26. Egsgaard, H. and Carlsen, L., *Org. Mass Spectrom.*, 1989, vol. 24, p. 1031.
27. Khrapkovskii, G.M., Ermakova, E.A., and Rafeev, V.A., *Izv. Ross. Akad. Nauk, Ser. Khim.*, 1994, no. 12, p. 2118.